Accelerated Localized Correlated Spectroscopy with Compressed Sensing Reconstruction Using Joint Hankel Low Rank Regularization and Group Sparsity

Andres Saucedo[1], Manoj K. Sarma[1], and M. Albert Thomas[1]

[1]Radiological Sciences, University of California, Los Angeles, Los Angeles, CA, United States

Synopsis

Compressed sensing (CS) combined with non-uniform undersampling, such as the low-rank Hankel matrix completion method, have accelerated the acquisition time of 2D magnetic resonance spectroscopy (MRS). This technique relies on reconstructing the vector of all t_1 points separately for each F_2 point. We introduce a CS-based method that implements joint Hankel low rank regularization, which enforces the low-rankness of all Hankel matrices formed from the entire F_2-t_1 data simultaneously. We compare this method with group sparsity CS reconstruction of retrospectively undersampled localized correlated spectroscopy (COSY) acquisitions in a brain phantom and calf muscle.

Introduction

One-dimensional magnetic resonance spectroscopic (MRS) techniques allow site-specific measurements of metabolite compositions to probe the impact of various pathologies non-invasively. One of the main limitations of 1D techniques is the overlap of spectral peaks. Two-dimensional spectroscopy (2D MRS) can differentiate overlapping peaks but requires an increase in scan time proportional to the number of measured t_1 points needed to resolve the additional spectral dimension F_1[1,2]. Acceleration methods that combine non-uniform under-sampling (NUS) of t_1 with compressed sensing (CS) reconstruction have been proposed to reduce the scan time[3,4]. CS methods based on group sparsity (GS) have been applied for accelerated 2D correlated spectroscopy (COSY) and shown to outperform maximum entropy and conventional CS reconstruction[5,6]. Recently, low-rank Hankel matrix completion, which exploits the low rank property of the Hankel matrix formed from all t_1 measurements corresponding to any point along F_2, has been proposed as an alternative method that can more accurately recover broad peaks compared to l_1-norm based CS methods[7]. This technique relies on reconstructing the vector of all t_1 points separately for each F_2 point[7,8]. In this study, we introduce a CS-based method that implements joint Hankel low rank (JHLR) regularization, which enforces the Hankel low-rankness of all matrices formed from the entire F_2-t_1 data simultaneously. We compare this method with GS reconstruction of retrospectively undersampled brain phantom and calf-muscle localized correlated spectroscopy (L-COSY) acquisitions.

Methods

The reconstruction of the F_2-t_1 data x using JHLR regularization is posed as the following minimization problem:

$$\min_{x \in \mathbb{C}^{N_2 \times N_1}} \frac{1}{2}\|y - Ax\|_2^2 + \tau \sum_{n=1}^{N_2} \|H_n x\|_{S_1}$$

where y is the under-sampled F_2-t_1 data, A is the undersampling operator, N_1 the number of F_1 points, N_2 the number of F_2 points, $\|\cdot\|_{S_1}$ denotes the Schatten 1-norm[9] , τ is a regularization parameter, and H_n is the operator that forms a Hankel matrix from all t_1 measurements corresponding to the n^{th} F_2 point of x. The regularization parameters for each algorithm were chosen empirically as those minimizing the normalized root mean square error (nRMSE) for selected diagonal and cross peaks. Both the JHLR and GS algorithms are based on the alternating direction method of multipliers (ADMM)[10,11]

A COSY spectrum of a brain phantom composed of several metabolites at physiological concentrations was acquired with the following parameters: VOI = 3x3x3 cm^3, TR=2 s, TE=30 ms, 1024 t_2 points, 128 t_1 points, BW_2=2000 Hz, BW_1=1250 Hz, and 12 averages. A COSY spectrum of the soleus calf muscle from a healthy volunteer was acquired with: VOI = 2.5x2.5x2.5 cm^3, TR=1.5 s, TE=30 ms, 1024 t_2 points, 96 t_1 points, BW_2=2000 Hz, BW_1=1250 Hz, and 8 averages. These data sets were retrospectively undersampled at reduction factors (RF) of 2, 2.5, 3, 3.5, 4, and 5 using NUS masks generated with a skewed sine bell squared sampling density function.

To assess reconstruction and quantitation accuracy, the peak integrals of the fully-sampled, GS-reconstructed, and JHLR-reconstructed spectra were computed, as well and the nRMSE's of selected diagonal and cross peaks. For the brain phantom the diagonal peaks are: N-acetylaspartate (NAA), Creatine (Cr-3.0), Choice (Ch-3.2), myo-Inositol (mI-3.2), and Cr-3.9; the cross peaks are: Alanine (Ala), Lactate (Lac), Threonine (Thr), glutamine/glutamate (Glx), N-acetylaspartate (NAA), Aspartate (Asp), and mI-Ch. For the calf muscle, the diagonal peaks are the $(CH_2)_N$ lipids, lipid methylene peaks, Cr-3.0, Ch-3.2, Cr-3.9, and the olefinic (CH=CH) peaks; the cross peaks are the extra- and intra-myocellular lipids ($EMCL_1$/$EMCL_2$ and $IMCL_1$/$IMCL_2$) and the triglyceride backbone fatty (TGBF) acids.

Results

In almost all cases, Table 2 shows that JHLR produces lower percent errors of the peak integrals compared to GS. Similarly, Table 1 shows that JHLR generally gives lower nRMSE values for most peaks at all reduction factors. Figures 1 and 2 demonstrate the comparable performance of GS and JHLR in reconstructing the calf and brain COSY spectra, although the difference maps indicate that JHLR recovers the spectra with higher reconstruction accuracy.

Discussion

Both JHLR and GS perform comparably in reconstructing the retrospectively undersampled brain phantom and calf muscle data. However, as seen by the absolute difference maps, peak integrals, and nRMSE values, JHLR results in the most accurate COSY reconstructions. Results indicate that this method is a competitive alternative to existing reconstruction techniques for accelerated localized 2D MRS.

Conclusion

This study has introduced a novel low-rank based regularization technique for accelerated 2D MRS. Compared with group sparsity-based CS reconstruction, JHLR regularization has shown greater accuracy quantitatively both in terms of peak integrals and nRMSE's of reconstructed peaks. Future work includes extending JHLR-based CS reconstruction to multi-dimensional 2D spectroscopic imaging.

Acknowledgements

Grant support NIH/NIBIB - 5R21EB020883-02

References

[1] Thomas, M.A., et al. Localized two-dimensional shift correlated MR spectroscopy of human brain. Magnetic Resonance in Medicine, 2001; 46(1): 58-67.

[2] Thomas, M.A., et al. Evaluation of two-dimensional L-COSY and JPRESS using a 3T MRI scanner: from phantoms to human brain in vivo. NMR in Biomedicine, 2003; 16(5):245-251.

[3] Furuyama, J.K., et al. Application of Compressed Sensing to Multi-dimensional Spectroscopic Imaging in human prostate. Magnetic Resonance in Medicine, 2012; 67(6):1499-1505.

[4] Wilson, N.E., et al. Accelerated Five-dimensional Echo Planar J-resolved Spectroscopic Imaging: Implementation and pilot validation in human brain. Magnetic Resonance in Medicine, 2016; 75(1):42-51.

[5] Burns, B.L., et al. Group Sparse Reconstruction of Multi-dimensional Spectroscopic Imaging in Human Brain in vivo. Algorithms, 2014; 7 (3):276-294.

[6] Burns, B.L., et al. Non-Uniformly under-sampled Multi-dimensional Spectroscopic Imaging in vivo: maximum entropy versus compressed sensing reconstruction. NMR in Biomedicine, 2014; 27(2):191-201.

[7] Qu, X., et al. Accelerated NMR Spectroscopy with Low-Rank Reconstruction. Angewandte Chemie International Edition, 2015; 54(3):852-854.

[8] Guo, D., et al. A Fast Low Rank Hankel Matrix Factorization Reconstruction Method for Non-Uniformly Sampled Magnetic Resonance Spectroscopy. IEEE Access, 2017; 5:16033-16039.

[9] Lefkimmiatis, S., et al. Hessian Schatten-norm Regularization for Linear Inverse Problems. IEEE Transactions on Image Processing, 2013; 22(5):1873-1888.

[10] Goldstein, T., Osher, S. The Split-Bregman Method for L1-regularized problems. SIAM Journal on Imaging Sciences, 2009; 2(2):323-343.

[11] Afonso, M.V., et al. An Augmented Lagrangian Approach to the Constrained Optimization Formulation of Imaging Inverse Problems. IEEE Transactions on Image Processing, 2011; 20(3):681-695.

Figures

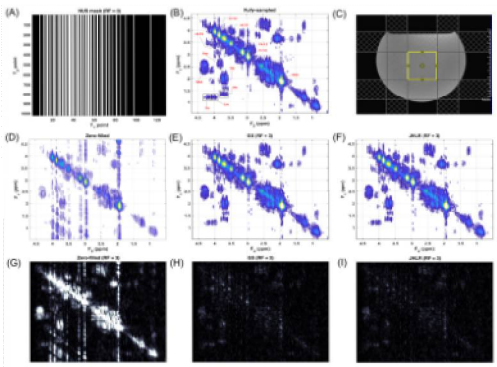

Figure 1: (A) NUS mask (RF = 3). (B) Fully-sampled COSY spectrum of brain phantom. (C) localization of brain phantom. (D) Zero-filled reconstruction (RF = 3). (E) Group sparse (GS) reconstruction. (F) Joint Hankel low-rank (JHLR) reconstruction. (G) absolute difference map (relative to the fully-sampled spectrum) of the zero-filled reconstruction. (H) absolute difference map of the GS reconstruction. (I) absolute difference map of the JHLR reconstruction. Note the lower intensity of the absolute difference map of JHLR. The absolute difference images are windowed and leveled identically.

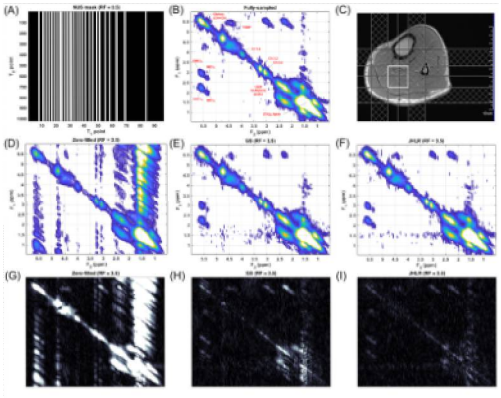

Figure 2: (A) NUS mask (RF = 3.5). (B) Fully-sampled COSY spectrum of calf muscle. (C) localization of soleus calf muscle. (D) Zero-filled reconstruction (RF = 3.5). (E) Group sparse (GS) reconstruction. (F) Joint Hankel low-rank (JHLR) reconstruction. (G) absolute difference map (relative to the fully-sampled spectrum) of the zero-filled reconstruction. (H) absolute difference map of the GS reconstruction. (I) absolute difference map of the JHLR reconstruction. Note the lower intensity of the absolute difference map of JHLR. The absolute difference images are windowed and leveled identically.

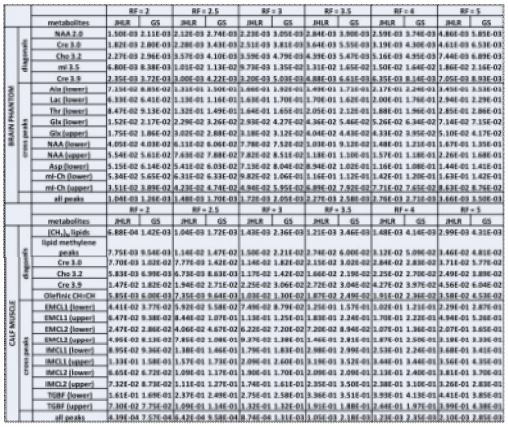

Table 1: Normalized root mean square error (nRMSE) values for brain phantom and calf muscle COSY reconstructions at various reduction factors (RF) for selected diagonal peaks and cross peaks. Note the lower nRMSE values of JHLR reconstruction compared to GS.

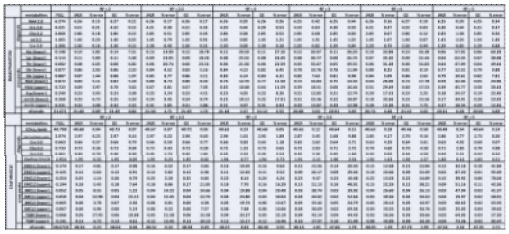

Table 2: Peak integral values for fully-sampled and reconstructed brain phantom and calf muscle COSY spectra at all reduction factors (RF) for selected diagonal and cross peaks. Note the general trend in lower percent errors of JHLR compared to GS. The peak integral values for the fully-sampled COSY are shown in the leftmost column.